Proceedings of the IASTED
International Conference on

PARALLEL AND DISTRIBUTED COMPUTING AND NETWORKS

Editor: M.H. Hamza

As part of the 22nd IASTED International Multi-Conference on
Applied Informatics

February 17 – 19, 2004
Innsbruck, Austria

A Publication of The International Association of
Science and Technology for Development – IASTED

ISBN: 0-88986-369-5 ISSN: 1027-2666

ACTA Press Anaheim • Calgary • Zurich

Proceedings of the IASTED International Conference on **Parallel and Distributed Computing and Networks**, held February 17 – 19, 2004, Innsbruck, Austria.

Sponsors

The International Association of Science and Technology for Development (IASTED)
- Technical Committee on Parallel and Distributed Computing and Systems

Conference Chair

M.H. Hamza

International Program Committee

Additional Reviewers

For each IASTED conference, the following review process is used to ensure the highest level of academic content. Each full manuscript submission is peer reviewed by a minimum of two separate reviewers on the International Program Committee/Additional Reviewers list. The review results are then compiled. If there is a conflict in reviews, the paper is sent to a third reviewer.

ACTA Press
P.O. Box 5124
Anaheim, CA 92814-5124
USA

ACTA Press
#80, 4500 - 16th Ave. NW
Calgary, AB T3B 0M6
Canada

ACTA Press
P.O. Box 354
CH-8053 Zurich
Switzerland

Publication Code: 420

TABLE OF CONTENTS
PDCN 2004

CLUSTER AND GRID COMPUTING

SCHEDULING AND RESOURCE ALLOCATION

MOBILE COMPUTING AND WIRELESS NETWORKS

COMPUTER NETWORKS AND COMMUNICATIONS

DISTRIBUTED ALGORITHMS AND SYSTEMS

FAULT TOLERANCE

PARALLEL COMPUTING

PARALLEL COMPUTING SYSTEMS

PARALLEL PROCESSING AND PROGRAMMING

RELIABILITY, PERFORMANCE EVALUATION, AND QOS

ROUTING AND INTERCONNECTION NETWORKS

WEB TECHNOLOGIES

PAPERS FROM OTHER IASTED CONFERENCES

ADDITIONAL PAPERS

Proceedings of the IASTED International Conference
PARALLEL AND DISTRIBUTED COMPUTING AND NETWORKS
February 17-19, 2004, Innsbruck, Austria

ADAPTIVE BEAM-FORMER GENERALIZED DETECTOR IN WIRELESS SENSOR NETWORKS

Vyacheslav Tuzlukov, Won-Sik Yoon, and Yong Deak Kim
Department of Electrical and Computer Engineering
College of Information Technology, Ajou University
San 5, Wonchon-dong, Paldal-gu, Suwon 442-749
Korea

ABSTRACT

This paper is concerned with a generalized detector (GD) constructed based on the generalized approach to signal processing (GASP) in noise and employed in wireless sensor networks. The GD decides if an observation contains a multidimensional signal belonging to one space or if it contains a multidimensional signal belonging to an orthogonal subspace when unknown complex Gaussian noise is present. We evaluate the performance of the generalized detector in both the matched and mismatched signal cases Our results show that for constant power complex Gaussian noise, if the signal is matched to the steering vector, the GD performance outperforms the adaptive matched filter (AMF), the generalized likelihood ratio test (GLRT), the adaptive coherence estimator (ACE), and the adaptive beam-former orthogonal rejection test (ABORT).

KEY WORDS
Adaptive detection, adaptive signal processing, array signal processing, adaptive side-lobe blanking.

1. INTRODUCTION

In this paper, we continue to develop the GASP [1-4] under specific conditions that are characteristics of wireless sensor networks. We consider the system using multiple antennas at both the transmitter and the receiver (sensors and sink). We will compare the detection algorithm based on the GASP with several other well-studied adaptive detection algorithms: AMF [5], GLRT [6], ACE [7,8], and ABORT [9]. According to the GASP, assume that we have a set of training signals $\mathbf{x}_k, k = 1,..., K$ in an N-dimensional complex space, which are characterized by a covariance matrix $\mathbf{R}$, which is unknown to us. Although $\mathbf{R}$ is unknown, we can estimate it by computing the sample covariance matrix $\mathbf{X}$

$$\mathbf{X} = \sum_{k=1}^{K} \mathbf{x}_k \mathbf{x}_k^H \quad , \tag{1}$$

where the superscript H denotes complex conjugate transpose.

We also assume that there is another set of noise samples $\mathbf{y}_k, k = 1,..., K$ in the same N-dimensional complex space with the sample covariance matrix $\mathbf{Y}$

$$\mathbf{Y} = \sum_{k=1}^{K} \mathbf{y}_k \mathbf{y}_k^H \tag{2}$$

with the same statistics $\mathbf{R}$ (for simplicity). It is known *a priori* that a "no" signal obtains in the noise samples $\mathbf{y}_k$ (the reference sample). The training signals $\mathbf{x}_k$ and noise samples $\mathbf{y}_k$ are uncorrelated. How we can do this is discussed in more detail in [2,3].

We are given another signal $\mathbf{x}$ belonging to the same set of training signals $\mathbf{x}_k$, which is corrupted by zero-mean complex Gaussian noise $\mathbf{n}$ with statistics characterized by $\mathbf{R}$. We assume that $\mathbf{x}$ may contain a signal proportional to the unit vector $\mathbf{s}$, with proportionality constant α. It may alternatively have some other disturbance proportional to $\mathbf{s}_\perp$, where $\mathbf{s}_\perp$ is any vector orthogonal to $\mathbf{s}$. We need to design a detection algorithm representing a compromise between good probability of detection for weak signals, low probability of false alarms due to strong signals perpendicular to $\mathbf{s}$ (side-lobe signals), invariance properties, efficient computation, etc.

This paper introduces GD under mentioned above initial conditions. In line with the GASP, GD is based on two-phase test, where the first test checks the hypothesis that a signal proportional to $\mathbf{s}$ is present, and, if we do not reject this hypothesis, the second test verifies detection. In doing so, the threshold both under the first phase and under the second phase is the same and is caused by the false alarm probability given before and the power spectral density of the GD background noise. Moreover, during the second phase a decision-making rule is based on estimation of the statistic test variance at the GD output.

2. INITIAL PREMISES

We search for targets in the presence of jamming and noise. Under designing the receiver, there is a compromise between a low gain wide beam that covers the area to be searched using relatively few pointing directions, versus a narrow beam, which can have higher gain in the target direction. Without high gain, the target might be obscured by receiver noise.

We desire that the detection algorithm could have low probability of detection for targets smaller than some defined size but have a high probability of detection for targets larger than some defined size. Between these two sizes, there must be a transition region, within which we can tolerate either high or low probability of detection. The region to be searched will be "tiled" by successively pointing the beam in various directions. The goal of the search is not only to detect a target but also to define its approximate direction, which is the beam pointing direction. The search must be considered unsuccessful if the target is detected while the beam is pointing elsewhere, but realistic antenna beams have side-lobes that are directions with relatively high gain outside the main beam. A strong target can sometimes trigger detection when it is located in a side-lobe direction, therefore appearing just like a somewhat weaker target in the main beam. This is a false alarm with system consequences not very different from reporting a target when there is only noise.

Since large targets are detectable with less antenna gain than small ones, the desirable beam shape should have adequately high gain in a certain defined angular region, adequately low gain outside a certain somewhat larger defined angular region, and transition region in between. For receivers adapted to jamming and other kind of interference, the considerations are similar, but not identical. We can no longer to know the beam shape because an adaptive antenna's beam will depend in detail on interference.

When results from N antennas are available to be combined, we usually consider the target and the beam in an N-dimensional complex space whose coordinates are the observations on the N antennas. Any hypothetical target will engender some predicted response in the N antenna elements, thereby appearing as a point in this "antenna space". This is so-called the target vector. Since the response of a larger target will be increased in the same proportions in all the antenna elements, the normalized target vector is a function of the direction of the target in space, whereas the length of the target vector depends also on the cross section of the target. For observations of an actual target corrupted by noise, the output SNR would be proportional to the squared length of the target vector.

Most algorithms for processing observations from an antenna array include a step that forms some linear combination (weighted sum) of the observations on the N antennas to give one scalar value. The weights used in such linear combination can be combined into vector we call the weight vector. It is important to recognize that a linear combination of observations from N separate antennas results in one synthetic antenna that has its own beam pattern.

The most important special case is the weight vector that would be used if the interference were spatially random, like receiver noise. This is called the steering vector and it is identical to a target vector for a target located at the center of the beam. The angle between a target vector and a steering vector in the antenna space is analogous to the angle between a target and a beam pointing direction in 3-D space.

3. GENERALIZED DETECTOR

The GD decides if a complex N-component test vector $\mathbf{x}$ contains a signal vector $\mathbf{s}$ or if $\mathbf{x}$ contains a signal $\mathbf{s}_{\perp}$ using the reference noise sample $\mathbf{y}_k$, where $\mathbf{s}_{\perp}$ is orthogonal to $\mathbf{s}$. A decision between two possible hypotheses is the following [2,3]:

- Orthogonal signal-in-noise hypothesis

$$H_0 : \begin{cases} \mathbf{x} = \alpha\, \mathbf{s}_{\perp} + \mathbf{n}; \\ \mathbf{y}_0 = \mathbf{n}_1; \end{cases} \tag{3}$$

- Signal-in-noise hypothesis

$$H_1 : \begin{cases} \mathbf{x} = \alpha\, \mathbf{s} + \mathbf{n}; \\ \mathbf{y}_0 = \mathbf{n}_1, \end{cases} \tag{4}$$

where $\mathbf{n}_1$ is the zero-mean complex Gaussian noise with statistic characterized by $\mathbf{R}$, α is an unknown complex scalar.

According to the GASP [1-4], the test statistic at the GD output for the hypothesis H_1 takes the form

$$\mathbf{Z}_G^{out} = \frac{2\mathbf{s}^{*H}\mathbf{X}^{-1}\mathbf{x} - \mathbf{x}^H\mathbf{X}^{-1}\mathbf{x} + \mathbf{y}^H\mathbf{Y}^{-1}\mathbf{y}}{\sqrt{\mathbf{s}^{*H}\mathbf{X}^{-1}\mathbf{s}}} > \gamma_G\,, \tag{5}$$

and vice versa for the hypothesis H_0, where $\mathbf{s}^*$ is the model signal (searching signal generated by the sensor antenna). We can define $\mathbf{x}_0 \equiv \mathbf{x} = \alpha\, \mathbf{s}_{\perp} + \mathbf{n}$ for the hypothesis H_0 and $\mathbf{x}_0 \equiv \mathbf{x} = \alpha\, \mathbf{s} + \mathbf{n}$ for the hypothesis H_1, respectively. Then, using (3) and (4), the statistic test (5) can be written in the following form in statistical sense: the hypothesis H_0

$$\mathbf{Z}_G^{out} = \alpha^2 \mathbf{s}_\perp \mathbf{s}^{*H} + 2\alpha^2 \mathbf{s}^* \mathbf{n}^H - 2\alpha^2 \mathbf{s}_\perp \mathbf{n}^H + \mathbf{n}_1 \mathbf{n}_1^H - \mathbf{n}\mathbf{n}^H \tag{6}$$

and the hypothesis H_1

$$\mathbf{Z}_G^{out} = \alpha^2 \mathbf{s}\mathbf{s}^{*H} + \mathbf{n}_1 \mathbf{n}_1^H - \mathbf{n}\mathbf{n}^H . \tag{7}$$

The great peculiarity of functioning GD is the following. At the fist phase of detection, we must satisfy the conditi-on $\mathbf{s}^* = 0$, i.e., the model signal is switched off. During the second phase, we ask whether the signal is more likely to lie in the one-dimensional subspace **s** or in the comple-mentary subspace $\mathbf{s}_\perp$, given that we expect it to be corru-pted by noise with covariance **R**, estimated by the sample covariance matrix **X**. By this reason, during the second phase, the model signal $\mathbf{s}^*$ is switched on and we should tend to approach that the condition $\mathbf{s}^* = \mathbf{s}$ would be satis-fied.

4. ANALYTICAL PERFORMANCE

Introduce the mismatch angle θ

$$\cos^2\theta \equiv \frac{|\mathbf{s}^{*H}\mathbf{R}^{-1}\mathbf{s}_m|^2}{(\mathbf{s}^{*H}\mathbf{R}^{-1}\mathbf{s}^*)(\mathbf{s}_m^H\mathbf{R}^{-1}\mathbf{s}_m)} . \tag{8}$$

In this context, the angle θ refers to the angle in the whi-tened space between the steering vector $\mathbf{s}^*$ used in the de-tector and the direction vector $\mathbf{s}_m$ of the signal in the test vector. We introduce the notation $\mathbf{s}_m$ for the signal direc-tion to distinguish it from the steering vector $\mathbf{s}^*$. Note that the direction vector $\mathbf{s}_m$ is aligned with the steering vector $\mathbf{s}^*$ under the hypothesis H_1 and orthogonal to the steering vector $\mathbf{s}^*$ under the hypothesis H_0. In general, the direction vector $\mathbf{s}_m$ has a component along the stee-ring vector $\mathbf{s}^*$ and a component along the orthogonal ve-ctor $\mathbf{s}_\perp$.

Explain, what we mean under the whitened space. We as-sume that the interference observations are individual po-ints in the *N*-dimensional antenna subspace. We can the-refore identify a linear transformation that could be appli-ed to the vectors observed on the antennas such that after such a transformation, the transformed interference appe-ars to be randomly distributed in *N*-dimensional space. We call this process of transformation whitening the data. The whitened data is not necessarily computed in the act-ual wireless sensor network system. It is an artifice used to analyze the performance of the wireless sensor network system. Consequently, we may use the target vectors and steering vectors in the whitened space instead of antenna space. However, we cannot to define a search time or a detection probability because we do not know the actual interference. We can use the whitened space to compare different wireless sensor network systems.

The detectable signal-to-interference-plus-noise ratio (SINR) is determined by

$$q_\theta \equiv |\alpha|^2 \cdot \mathbf{s}_m^H \mathbf{R}^{-1}\mathbf{s}_m \cdot \cos^2\theta . \tag{9}$$

Recall that α is the complex scalar in (3) and (4). In our definition, we assume that both the direction vector $\mathbf{s}_m$ and the steering vector $\mathbf{s}^*$ have unit norm, i.e.,

$$\mathbf{s}_m^H\mathbf{s}_m = \mathbf{s}^{*H}\mathbf{s}^* = 1 .$$

Since the detector is "steered" in the $\mathbf{s}^*$ direction and the signal emanates from the $\mathbf{s}_m$ direction, only a fraction of the total available SINR

$$|\alpha|^2 \cdot \mathbf{s}_m^H\mathbf{R}^{-1}\mathbf{s}_m$$

is usable by the detector. The quantity q_θ represents that usable fraction, assuming **R** was known *a priori*. The SINR lost due to signal mismatch is determined by

$$\tilde{q}_\theta \equiv |\alpha|^2 \cdot \mathbf{s}_m^H \mathbf{R}^{-1}\mathbf{s}_m \cdot \sin^2\theta . \tag{10}$$

It is easily seen that the total available SINR equals the sum of q_θ and $\tilde{q}_\theta$.

With these definitions, we proceed with the performance analysis for the GD. We begin by deriving an expression for the mismatched probability of detection $P_D(\theta)$, which is defined as the probability of choosing the hypothesis H_1 for a signal with the mismatch angle θ

$$P_D(\theta) \equiv \Pr[H_1 \mid \theta] . \tag{11}$$

We obtain our expression for $P_D(\theta)$ of the GD from the probability distribution function $f_\theta(\mathbf{Z})$ of the test statis-tic $\mathbf{Z}_G^{out}$ parameterized by the mismatch angle θ. Recall from (5) that we choose the hypothesis H_1 when $\mathbf{Z}_G^{out} > \gamma_G$; hence

$$P_D(\theta) = \int_{\gamma_G}^{\infty} f_\theta(\mathbf{Z})\, d\mathbf{Z} . \tag{12}$$

To evaluate the integral in (12), we introduce the loss fac-tor β_θ whose distribution is known and can be evaluated.

The loss factor β_θ can be determined by the following form:

$$\beta_\theta \equiv \frac{\mathbf{s}^{*H}\mathbf{X}^{-1}\mathbf{s}_m}{\mathbf{s}^{*H}\mathbf{X}^{-1}\mathbf{s}_m + (\mathbf{s}^{*H}\mathbf{X}^{-1}\mathbf{s}_m)(\mathbf{x}^{H}\mathbf{X}^{-1}\mathbf{x}) - |\mathbf{s}^{*H}\mathbf{X}^{-1}\mathbf{x}|^2} . \tag{13}$$

We use a subscript θ to indicate the mismatch angle between the signal vector $\mathbf{s}_m$ in the input data $\mathbf{x}$ and the steering vector $\mathbf{s}^*$, as defined in (8).

Under the hypothesis H_0, $\theta = 90^\circ$, and under the hypothesis H_1, $\theta = 0^\circ$. In [10], it is shown that the loss factor β_θ is distributed as a complex non-central beta random variable whose probability distribution function may be expressed in the following form

$$f(\beta_\theta) = e^{-s_\theta \beta_\theta} \sum_{Z=0}^{K-N+2} \binom{K-N+2}{Z} \frac{K!}{(K+Z)!} \times s_\theta^Z f_{K-N+2,N-1+Z}(\beta_\theta), \quad 0 \le \beta_\theta \le 1, \tag{14}$$

where $f_{n,m}(\beta)$ is the probability distribution function of a complex central beta random variable as follows:

$$f_{n,m}(\beta) \equiv \frac{(n+m-1)!}{(n-1)!(m-1)!} \beta^{n-1}(1-\beta)^{m-1}, \quad 0 \le \beta \le 1. \tag{15}$$

We can express the probability distribution function $f_\theta(\mathbf{Z})$ in terms of the conditional probability distribution function

$$f_\theta(\mathbf{Z}) = \int_0^1 f_\theta(\mathbf{Z} \mid \beta_\theta) \cdot f(\beta_\theta)\, d\beta_\theta . \tag{16}$$

We substitute (16) into the expression for the mismatched probability of detection $P_D(\theta)$ in (11) and reverse the order of integration to obtain

$$\begin{aligned} P_D(\theta) &= \int_0^1 \left[\int_{\gamma_G}^{\infty} f_\theta(\mathbf{Z} \mid \beta_\theta)\, d\mathbf{Z} \right] \cdot f(\beta_\theta)\, d\beta_\theta \\ &= \int_0^1 P_D(\theta) \mid \beta_\theta \cdot f(\beta_\theta)\, d\beta_\theta , \end{aligned} \tag{17}$$

where we introduce the notation $P_D(\theta) \mid \beta_\theta$ to represent the mismatched probability of detection for the GD conditioned on β_θ. We evaluate $P_D(\theta) \mid \beta_\theta$ in the following form

$$\begin{aligned} P_D(\theta) \mid \beta_\theta &= \int_{\gamma_G}^{\infty} f_\theta(\mathbf{Z} \mid \beta_\theta)\, d\mathbf{Z} \\ &= 1 - \int_{-\infty}^{\gamma_G} f_\theta(\mathbf{Z} \mid \beta_\theta)\, d\mathbf{Z} . \end{aligned} \tag{18}$$

The integral on the last line of (18) can be expressed as the cumulative distribution function of the complex non-central F-distribution, which is expressible in many forms. A convenient form given in [10] uses the following finite sum expression:

$$P_D(\theta) \mid \beta_\theta = 1 - \frac{1}{\tau_\theta^{K-N+1}} \sum_{m=0}^{K-N+1} \binom{K-N+1}{m} \times (\tau_\theta - 1)^m G_m\left(\frac{\delta_{\beta_\theta}^2}{\tau_\theta}\right), \tag{19}$$

where

$$\tau_\theta = 1 + \gamma_G - \beta_\theta , \tag{20}$$

$$\delta_{\beta_\theta}^2 = q_\theta \cdot \beta_\theta , \tag{21}$$

and the function $G_m(x)$ is defined in terms of the incomplete Gamma function $\Gamma(m, x)$ as follows:

$$G_m(x) \equiv \frac{\Gamma(m,x)}{(m-1)!} = e^{-x} \sum_{n=0}^{m-1} \frac{x^n}{n!} . \tag{22}$$

In the performance examples presented below, we evaluate the mismatched probability of detection $P_D(\theta)$ with numerical integration techniques for the integral in (17) along with the finite sum expressions given in (15), (19)–(21).

The analytical expression for the probability of detection for a matched signal is obtained by substituting $\theta = 0$ into (17). For this case, the distribution of the loss factor β_0 given by (13) reduces to the central beta density whose probability distribution function is given in (15).

The probability of false alarm P_{FA} for the GD is defined in this context as the probability of selecting the signal-in-noise hypothesis H_1 when SINR=0, i.e., $\alpha = 0$. We obtain the analytical expression for the probability of false alarm from (17) by setting $\alpha = 0$. Hence, the probability of false alarm P_{FA} is as follows

$$P_{FA} = \int_0^1 P_{FA} \mid \beta_0 \cdot f(\beta_0)\, d\beta_0 , \tag{23}$$

where $P_{FA} \mid \beta_0$ is the probability of false alarm conditioned on the loss factor β_0. Setting the condition $\alpha = 0$ implies the condition $\delta_{\beta_\theta} = 0$, and it follows that

$$G_m\left(\frac{\delta^2_{\beta_\theta}}{\tau_\theta}\right) = G_m(0) = 1. \qquad (24)$$

After substituting (24) in (19) and using the binomial theorem, we obtain the following:

$$P_{FA} \mid \beta_0 = \tau_0^{-K+N-1}. \qquad (25)$$

5. COMPUTER SIMULATION RESULTS

In this section, we show performance curves for the GD algorithm and relate it to the AMF, GLRT, ACE, and ABORT detection algorithms. We compare the probability of detection for the case when the signal $\mathbf{s}_m$ in the test vector $\mathbf{x}$ is aligned with the steering vector $\mathbf{s}^*$ (case of the matched detection performance) and the case when the signal $\mathbf{s}_m$ in the test vector $\mathbf{x}$ is misaligned with the steering vector $\mathbf{s}^*$ (case of the mismatched performance).

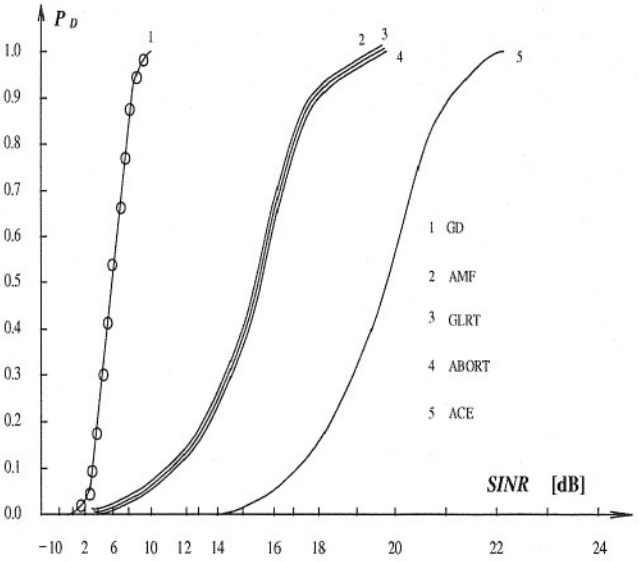

Figure 1. Detection performances versus SINR for GD, AMF, GLRT, ABORT, and ACE.

We use the mismatch angle θ to designate the angle between the signal $\mathbf{s}_m$ in the test vector $\mathbf{x}$ and the steering vector $\mathbf{s}^*$ in the whitened N-dimensional data space. All performance curves for the GD algorithm are generated with numerical integration techniques and independently confirmed by Monte Carlo simulation.

The example we consider assumes a system of dimension $N = 5$ and $K = 25$ training vectors, and we choose the detection threshold for the GD test such that the average probability of false alarm in a noise only environment is $P_{FA} = 10^{-4}$.

Figures 1 and 2 represent the detection performances for the AMF, ACE, GLRT, ABORT, and GD algorithms. For independent confirmation, we also show results for the GD from 10 000 independent Monte Carlo trials. These simulated results are shown as circles in Figs. 1 and 2.

Figure 1, which is the matched detection performance, represents a slice of the constant probability of detection $P_D(\theta)$ contours at the condition $\cos^2\theta = 1$. Notice that the ACE detector has the lower probability of detection $P_D(\theta)$ than other four tests. The GD algorithm greatly outperforms the AMF, CLRT, and ABORT detectors. If we measure detection loss at the level equal to $P_D(\theta) = 0.5$ then for the noise model considered in this work, the AMF, GLRT, and ABORT detectors suffer about a 12 dB loss in SINR relative to the GD. The ACE detector suffers about 18 dB loss in SINR relative to the GD. In addition, note that the detection performance for the GD algorithm outperforms the detection performances for AMF, GLRT, ABORT, and ACE detectors for all values of SINR.

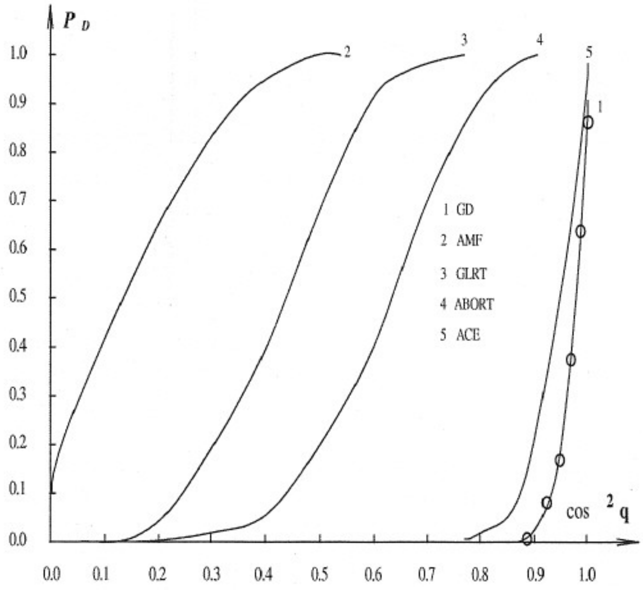

Figure 2. Detection performances versus $\cos^2\theta$ for GD, AMF, GLRT, ABORT, and ACE.

Figure 2 represents a slice of the constant probability of detection $P_D(\theta)$ contours under the condition SINR=20 dB. The performance at the left end of the plot $\cos^2\theta =$ 0 represents signals that are orthogonal to the steering vector $\mathbf{s}^*$ in the whitened data space. Similarly, the performance at the right end of the plot $\cos^2\theta = 1$ represents signals that are matched (or parallel) to the steering vector $\mathbf{s}^*$ in the whitened data space. We observe that the AMF detector has the least mismatch discrimination capabilities, whereas the GD algorithm is most selective. Only the ACE detector is relatively close to the GD detection performance.

6. CONCLUSION

We have developed and analyzed the GD algorithm for the considered noise model, which can be efficiently implemented as part of a two-phase detector. We have demonstrated that assuming a constant power multivariate Gaussian noise process, the GD algorithm has matched signal detection performance outperforming the AMF, GLRT, ABORT, and ACE detection algorithms. Furthermore, we have demonstrated that the GD algorithm has the best mismatch discrimination capabilities in comparison with the ACE, ABORT, GLRT, and AMF detectors. The GD algorithm provides an alternative detection strategy in the unknown multi-channel noise environment. When faced with the tradeoff between matched signal detection versus mismatched signal rejection, the GD algorithm ensures the best matched signal detection performance as well as the best side-lobe rejection performance relative to the AMF, GLRT, ABORT, and ACE detectors.

7. ACKNOWLEDGMENT

This work was supported in part by participation within the limits of the project "A Study on Wireless Sensor Networks for Medical Information" sponsored by IITA, Korea.

REFERENCES

[1] V.P. Tuzlukov, *Signal processing in noise: a new methodology* (IEC: Minsk, 1998).

[2] V.P. Tuzlukov, A new approach to signal detection, *Digital Signal Processing: A review Journal 8* (3), 1998, 166-184.

[3] V.P. Tuzlukov, *Signal detection theory* (Springer-Verlag: New York, 2001).

[4] V.P. Tuzlukov, *Signal processing noise* (CRC Press: Boca Raton, FL, 2002).

[5] F.C Robey, D.R. Fuhrmann, E.J. Kelly, and R.A. Nitzberg, A CFAR adaptive matched filter detector, *IEEE Trans., AES-28* (1), 208-216.

[6] E.J. Kelly, An adaptive detection algorithm, *IEEE Trans., AES-22* (3), 115-127.

[7] L.L Scharf and L.T. McWhorter, Adaptive matched subspace detectors and adaptive coherence estimators: *Proc. 30th Asilomar Conf. Signals, Syst., Comput.,* Pacific Grove, CA, 1996, 1114-1117.

[8] S. Kraut and L.L Scharf, The CFAR adaptive subspace detector is a scale-invariant GLRT, *IEEE Trans., SP-47* (9), 2538-2541.

[9] N.B. Pulsone and C.M. Rader, Adaptive beamformer orthogonal rejection test, *IEEE Trans., SP-49* (3), 521-529.

[10] E.J. Kelly, Adaptive detection in nonstationary interference–Part III, *Tech. Rep. 761,* Lincoln Lab., Mass. Inst. Technol., Lexington, MA, 1987.